GSI

Report 2008 - 03
März

Ion Beam Polarization in Storage Rings: Production, Controlling and Preservation

A. Prozorov, L. Labzowsky, G. Plunien,
D. Liesen, F. Bosch,
S. Fritzsche, A. Surzhykov

Gesellschaft für Schwerionenforschung mbH
Planckstraße 1 · D-64291 Darmstadt · Germany
Postfach 11 05 52 · D-64220 Darmstadt · Germany

Ion Beam Polarization in Storage Rings: Production, Controlling and Preservation

A. Prozorov[1], L. Labzowsky[1,2], G. Plunien[3], D. Liesen[4,5], F. Bosch[4], S. Fritzsche[4,5,6], A. Surzhykov[6]
[1]V.A. Fock Research Institute for Physics,
St. Petersburg State University,
198904 St. Petersburg, Russia
[2]St. Petersburg Nuclear Physics Institute,
188300 Gatchina, St. Petersburg, Russia
[3]Institute of Theoretical Physics, Dresden Technical University,
Mommsenstrasse 13, 01062 Dresden, Germany
[4]Gesellschaft für Schwerionenforschung mbH,
Planckstrasse 1, 64291 Darmstadt, Germany
[5]Institute of Physics, Heidelberg University,
Philosophenweg 12, 69120 Heidelberg, Germany
[6]Max-Planck Institut of Nuclear Physics,
Saupfercheckweg 1, 69117 Heidelberg, Germany

March 3, 2008

Abstract

The present paper reports on the actual status of the theoretical concepts for the production of polarized heavy ion beams in storage rings and for methods to control online the degree of polarization as well as investigations of the preservation of the polarization during the ion movement across the magnetic system of the ring. It is argued that for hydrogen-like ions beam polarization can be built up efficiently by optical pumping of the Zeeman sublevels of ground-state hyperfine levels and that the maximal achievable nuclear polarization exceeds 90%. Of special interest are polarized helium-like ions which can be produced by the capture of one electron, because in selected cases parity nonconservation effects are found to be of unprecedented size in Atomic Physics. The measurements of these effects require online-diagnostics of the degree of the ion beam polarization. It is shown that this can be accomplished by an online-detection of the linear polarization of the x-rays which are emitted with the capture of the electron. In order to investigate the preservation of the polarization of the ions stored in the ring, the concept of an instantaneous quantization axis is introduced. The dynamics of this axis and the behaviour of the polarization with respect to it are explored in detail.

Contents

1 Motivation: parity nonconservation (PNC) experiments in Atomic Physics

During the last few decades, experiments with spin-polarized particles (e.g.electrons and protons) have stimulated considerably many areas in basic research and applications [1]. While for electrons, protons and light ions, various techniques are known to obtain particle beams with a high degree of polarization, polarized beams of highly charged ions (HCI) are not yet available. However, intensive and polarized HCI beams are anticipated for the new GSI heavy-ion facility [2] and needed for many purposes, including tests of fundamental theories like parity nonconservation (PNC), validity of the Standard Model (SM) in the low-energy limit and particularly the time-reversibility. The latter problem was discussed recently in [3, 4] and it was argued that beams of heavy, bare polarized nuclei would be necessary for the observation of the effect. Here, we will concentrate on the applications of polarized HCI beam techniques for the search of PNC effects.
The search for PNC effects in atomic physics started immediately after the formulation of the Neutral Weak Current Hypothesis [5, 6, 7] which led afterwards to the foundation of the Standard Model. The first proposals concerned the optical dichroism in the Cs atom [8] and the optical rotation in Bi atom vapor [9]. The first successful experiment on the PNC observation in atoms was performed in Novosibirsk [10] with Bi atoms and the most accurate results have been obtained by the Boulder group with Cs atoms [11, 12].
A detailed theoretical description of the PNC effects in atoms can be found in [13]. A comprehensive modern review of the subject is given in [14]. PNC effects in atoms can be observed as different types of asymmetries in atomic transitions. A general expression for the one-photon transition probability including PNC effects reads

$$w = w_0 \left[1 + Re\xi_1(\vec{s}_p\vec{n}) + Re\xi_2(\vec{\gamma}\vec{n}) + Re\xi_3(\vec{h}\vec{n})\right] \tag{1}$$

Here, w_0 is the transition rate for the basic transition without PNC effects (usually a forbidden magnetic dipole transition M1 for reasons which will be explained in chapter 1.1), $\vec{n}$ the direction of the photon emission, $\vec{s}_p$ the photon spin, $(\vec{s}_p\vec{n}) = \pm 1$ the photon helicity which corresponds to a right (left) circular polarization, $\vec{\gamma}$ the electron polarization, and $\vec{h} = \vec{H}/|\vec{H}|$, where $\vec{H}$ is an external magnetic field.
In the absence of the PNC effects, the transition probability is a scalar; with the PNC included it acquires pseudoscalar corrections. The direction of the photon emission $\vec{n}$ is an ordinary (polar) vector. In Eq. (1) $\vec{n}$ is combined with all available pseudovectors (axial vectors) $\vec{s}_p, \vec{\gamma}$ and $\vec{h}$, to build up the possible pseudoscalar corrections to the probability with the coefficients ξ_1, ξ_2, and ξ_3. A scalar product of an ordinary vector and a pseudovector gives a pseudoscalar. The first pseudoscalar correction to the probability in Eq. (1) always exists, the second one arises only in the case of polarized electrons (in atoms or ions) and for the third one the presence of an external magnetic field is necessary.

1.1 PNC effects with circularly polarized photons

The expression (1) arises as a result of the mixing of atomic states with opposite parity by the effective weak PNC interaction which stems from the existence of the neutral currents. In the standard approximation where only one neighboring state with opposite parity and lying closest to the decaying level is taken into account, the coefficient ξ_1 in Eq. (1) is given by

$$\xi_1 = \frac{-i < \hat{H_w} >}{\Delta E - \frac{i}{2}\Gamma} R \tag{2}$$

Here, $< \hat{H_w} >$ is the non-diagonal (pure imaginary) matrix element of the effective PNC interaction between the electron and the nucleus. This interaction mixes levels with opposite parity (usually s and p states). The energy interval ΔE is the interval between the levels mixed by the PNC interaction and Γ is the sum of both the level widths; usually, the width Γ_p is much larger than Γ_s. The factor R will be discussed later.

The nuclear-spin-independent part of the effective electron-nucleus interaction Hamiltonian within the relativistic (Dirac) theory reads in relativistic units ($\hbar$ = c = 1)

$$\hat{H_w} = -\frac{G_F}{2\sqrt{2}} Q_w \rho_N(\vec{r}) \gamma_5 \tag{3}$$

where G_F is the Fermi constant, Q_w the "weak charge" of the nucleus, $\rho_N(\vec{r})$ the nuclear density distribution, and γ_5 the relativistic pseudoscalar Dirac matrix.

The Fermi constant is dimensional and equals

$$G_F \approx 10^{-5} \frac{1}{m_p^2} \tag{4}$$

where m_p is the proton mass. Actually, $10^5 m_p^2 \approx m_z^2$, where m_z is the mass of the neutral Z-boson according to the Standard Model. The interaction Hamiltonian in Eq. (3) is the result of the exchange of a Z-boson between the atomic electron and the nucleus.

In the matrix element $< \hat{H_w} >$ the Fermi constant arrives in the combination $m^2 G_F \approx 10^{-5}(m/m_p)^2$, where m is the mass of the electron. The smallness of this combination ($\sim 10^{-11}$) defines mainly the usual smallness of the PNC effects in atoms and ions.

The weak charge of the nucleus is defined as

$$Q_w = Z(1 - 4\sin^2\Theta_w) - N \tag{5}$$

where Z, N are the numbers of protons and neutrons in the nucleus and Θ_w is the Weinberg angle, which is the free parameter of the Standard Model. From high-energy experiments follows the value $\sin^2\Theta_w \simeq 0.23$. Therefore, the contribution of the neutrons to Q_w becomes dominant.

There exists also a nuclear-spin-dependent part $\hat{H'_w}$ of the PNC weak interaction between the electron and the nucleus. This interaction behaves like a parity-nonconserving hyperfine interaction. It contains another weak interaction constant, different from Θ_w and is suppressed by the factor $(1 - 4\sin^2\Theta_w)$. However, as was found in [15], the contribution of $\hat{H'_w}$ is always screened by the electromagnetic interaction $\hat{H_a}$ of the atomic electron with the anapole moment of the nucleus. The existence of the anapole moment was predicted in [16] and arises due to the weak interaction between the nucleons inside the nucleus. The interactions $\hat{H'_w}$ and $\hat{H_a}$ have exactly the same form and differ only by constants. Since the nucleon-nucleon interaction is stronger than the electron-nucleon one, the $\hat{H_a}$ interaction dominates the $\hat{H'_w}$ interaction. The only exception is the hydrogen atom, where the $\hat{H_a}$ interaction is absent. In heavy atoms the $\hat{H_a}$ contribution amounts to only about 1 % of the total $\hat{H_w}$ contribution.

Finally, the factor R in Eq. (2) represents the ratio

$$R = (\frac{w_1}{w_0})^{1/2} \tag{6}$$

where w_1 is the transition rate for the PNC transition opened due to the admixture of a state with opposite parity (usually a p-state) to the basic decaying state (usually an s-state). Thus, w_1 usually corresponds to an E1 transition and w_0 to an M1 transition. It is assumed that both transitions are going to the ground state (usually an s-state).
All the correction terms in Eq (1) arise due to the interference between the basic (M1) and the PNC (E1) amplitudes; this explains the square root in Eq. (6). A contribution proportional to w_1, i.e. quadratic in the weak interaction matrix element, can always be neglected.

1.2 PNC effects in atoms: enhancement factors

Usually, the PNC effects in atoms would never be observable due to the smallness of the constant $m^2 G_F \sim 10^{-11}$. Moreover, the matrix $\gamma_5 = -\binom{OI}{IO}$, where I is the unit 2x2 matrix, mixes the upper and lower components of the Dirac wave function $\psi = \binom{\varphi}{\chi}$. For low Z, the lower component χ is small compared to φ since $\chi \sim (\alpha Z)\varphi$, where $\alpha \simeq 1/137$ is the fine structure constant. In the point-nucleus limit the nuclear density distribution $\rho_N(\vec{r})$ in Eq. (3) can be replaced by the delta-function $\delta(\vec{r})$. Then the matrix element $< \hat{H}_w >$ is proportional to $|\psi(0)|^2$. For low Z, this would finally lead to a negligibly small influence of the PNC effect of the order $\alpha^2 m^2 G_F \approx 10^{-16}$.
However, several reasons lead to a strong enhancement of the PNC effects in heavy atoms and particularly in heavy HCI. These reasons were first formulated in [8, 9]. First, the matrix elements $< \hat{H}_w >$ are strongly dependent on Z. For HCI $< \hat{H}_w > \sim Z^5$ and this dependence can be explained by the following. The value of $|\psi(0)|^2$ is proportional to Z^3, an additional power of Z comes from the relation $\chi \sim (\alpha Z)\varphi$ and, finally, Q_w is roughly proportional to N and thereby also to Z. In heavy neutral atoms, only the valence electrons are responsible for the PNC effects. For these electrons, the electron density at the nucleus is screened by the other electrons so that $|\psi(0)|^2 \sim Z$. Consequently, for heavy neutral atoms $< \hat{H}_w > \sim Z^3$. For high Z atoms this enhancement is still essential. Second, the factor R is usually large (R >> 1) since the transition rate for E1 is larger than for M1 transitions. In neutral atoms, where the M1 transition is forbidden in the nonrelativistic limit one has to switch on an additional electric field to open it [8]. In HCI, where M1 transitions are always opened due to strong relativistic effects, the factor R is not so large.
Third, and most important, it follows from Eq. (2) that the energy denominator should be made as small as possible. From this point of view, a PNC experiment with neutral hydrogen where the 2s and 2p levels are almost degenerate and splitted only by small QED effects (Lamb-shift), would be desirable. The idea of such an experiment was discussed in [17, 18]. In heavy neutral atoms the s and p levels are no more degenerate so that the energy denominator is not small. The same holds true for H-like HCI where the s and p levels are again splitted only by the Lamb-shift, which exhibits a strong Z dependence ($\sim Z^4$) and, therefore, grows up very fast. For very high Z values the total enhancement factor converges to $Z\alpha^{-2}$ which unfortunately is not big enough to compensate the smallness of $m^2 G_F$.
However, for He-like HCI there is another possibility to profit from a small energy denominator in order to enhance the PNC effect: This is the "crossing" of energy levels with opposite parity. The behavior of the different levels of the first excited configurations is different with respect to Z. Some levels grow up faster, some slower within certain Z intervals. This can lead to "crossings" of the levels and, in particular, to crossings of levels with opposite parity at certain Z values. These "crossings" are not literal since Z takes only integer values, but they may correspond to very small values of ΔE. The most familiar example is provided by the 2^1S_0 and 2^3P_0

levels which cross twice: at Z = 64 and at Z = 92. The near-crossing of the 2^3S_1 and 2^3P_0 levels at Z = 32 is also known. The idea to use the level-crossing in He-like HCI for the search of PNC effects was introduced for the first time already in 1974 [19]. Later, this subject has been investigated theoretically in [20, 21, 22, 23, 24] and various types of experiments with HCI have been proposed. More details about the level crossings in He-like HCI in context with PNC effects can be found in [25].

1.3 PNC effects in neutral atoms: present status

In the Cs experiment [11] the 6s-7s excitation by right and left circularly polarized laser light is employed. The admixture of the 7p to the 7s level and of the 6p to the 6s level produces a PNC effect. The effect is observed via the fluorescence light from the 7s-6p transition; the transition probabilities are different for the right- and left-laser excitations due to the difference in the 7s level population. The population is different because the absorption rates are different for the right- and left-laser excitation.
The basic 6s-7s transition is a strongly forbidden M1 transition; it opens only due to relativistic effects of the order α^2 in the amplitude, i.e. α^4 in the probability. So, in the experiment it was not possible to observe this basic transition. Therefore, a weak electric field was applied that opened the 6s-7s M1 transition due to an admixture of the 6p and 7p levels to 6s and 7s just as in case of a PNC admixture. Then the PNC effect could be observed as an interference between the electric field-admixed E1 transition and the PNC-admixed E1 transition. The expected order of magnitude of the PNC effect observed, namely the asymmetry in the number of photons for right- and left-laser excitation was

$$\xi_1 \simeq 10^{-4}$$

and was finally measured with an accuracy of about 0.5 %. This accuracy allows the separation of the contribution of the anapole moment.
However, the experiment is not direct. To extract the information about the weak interaction constants (the weak charge Q_w and the anapole moment of the nucleus) from the experimental data, the theoretical calculation of the PNC effect in the neutral Cs atom is necessary. This calculation presents a very difficult task and the results of the calculations changed many times as a consequence of the inclusion of new corrections (see the history of these calculations which covers nearly one decade in [14]). First of all, a very accurate calculation of the wave functions for the Cs atom is necessary which takes into account the electron correlation at the accuracy level of 0.1 % . Such functions, obtained by different theoretical methods (Multiconfigurational Dirac-Hartree-Fock Expansion, Relativistic Many-Body Perturbation Theory, Relativistic Coupled Cluster Expansion) are presently available. Still the situation remains very precarious, since the PNC effect is caused by the valence 6s electrons, and the size of the effect is proportional to the density of these electrons at the nuclear surface. Thus, all 55 electrons of the Cs atom are involved in the screening of the nuclear charge.
It was found that the relativistic Breit interaction also plays an important role in this screening. The inclusion of the Breit interaction into any theoretical method for the evaluation of the electron correlation makes it much more cumbersome. Moreover, it appeared that the result is sensitive to the inclusion of radiative QED corrections, since the operators corresponding to these corrections are singular in the vicinity of the nucleus and, hence, give an unexpectedly large contribution. The most accurate up-to-date calculation [26] together with the experimental result yields

$$Q_w^{(AP)} = -72.65(29)_{exp}(36)_{theor} \tag{7}$$

This Atomic Physics (AP) result should be compared with the High Energy (HE) result

$$Q_w^{(HE)} = -73.19(13) \tag{8}$$

Unlike the AP results, the HE results are direct and do not require complicated calculations.

At the moment, the AP and HE results seem to be compatible. However, the theoretical part of $Q_w^{(AP)}$ still cannot be considered as fully reliable. Therefore, experiments with atomic systems of a much simpler structure (e.g. He-like HCI) are highly desirable. The direct measurement of the constant ξ_1 with the heaviest HCI is not possible at the moment due to the lack of detectors for circularly polarized photons in the energy region of $\sim$ 100 keV.

1.4 PNC effects with polarized HCI

PNC effects with polarized ion beams were considered in [23, 24]. In [23], an experiment was proposed for the determination of Q_w in He-like Eu and in [24] a similar experiment was discussed where the anapole moment of the nucleus using He-like Gd ions could be measured.

In case of the Eu experiment, the constant $\xi_2 = \frac{3\lambda}{I+1}\xi_1$ would be measured, where λ is the degree of the beam polarization, and I the nuclear spin. This measurement consists of registrating the asymmetry of the photon emission with respect to the direction of the ion beam polarization. The idea of the experiment is based on the near-crossing of the 2^1S_0 and 2^3P_0 levels.

The level scheme for the first excited configurations in $^{151}_{63}Eu^{61+}$ ions ($Z = 63, I = 5/2$) is shown in Fig. 1.

The basic transition is the hyperfine quenched (HFQ) one-photon transition $2^1S_0 \rightarrow 1^1S_0 + \gamma$ namely $1s2s^1S_0$ + (HF mixing) $1s2s^3S_1 \rightarrow (1s^2)^1S_0 + \gamma(M1)$. The PNC-admixed transition is $1s2s^1S_0$ + (PNC mixing) $1s2p^3P_0$ + (HF mixing) $1s2p^3P_1 \rightarrow (1s^2)^1S_0 + \gamma(E1)$.

The calculated asymmetry in the photon emission with respect to the ion beam polarization is:

$$\xi_2 \simeq \lambda \cdot 10^{-4} \tag{9}$$

The level crossing actually occurs for Gd (Z = 64) where the spacing between the 2^1S_0 and 2^3P_0 levels is very small [27]: ΔE = (0.004 $\pm$ 0.74) eV. In this case, according to Eq. (2) $Re\frac{1}{\Delta E - \frac{i}{2}\Gamma} = \frac{\Delta E}{\Delta E^2 + \frac{1}{4}\Gamma^2}$ where Γ is the 2^3P_0 level width with $\Gamma_{2^3P_0}$ = 0.0016 eV. The minimum value of $Re\frac{1}{\Delta E - \frac{i}{2}\Gamma}$ corresponds to ΔE = 0.078 eV which gives $\xi_2^{min} \simeq \lambda \cdot 10^{-3}$, i.e. 10 times larger than in Eu. The maximum value, corresponding to $\Delta E = \Gamma$ = 0.0016 eV is ξ_2^{max} = 0.052. The latter result is unprecedented for PNC effects in atoms and ions, though the big deviation between ξ_2^{min} and ξ_2^{max} does not allow to draw definite conclusions about the weak interaction constants. However, the experimental situation in Gd^{62+} is not so favorable as in Eu^{61+}. The reason is that in Gd^{62+} the lifetime of the 2^1S_0 level defined by the 2E1 two-photon transition to the ground state is about one order of magnitude smaller than the lifetime of the 2^3P_0 level, which is determined by the HFQ E1 transition to the ground state. This supplies a strong background from $2^3S_0 \rightarrow 1^1S_0 + \gamma$ transitions in experiments with Gd^{62+}: the HFQ E1 $2^3P_0 \rightarrow 1^1S_0 + \gamma(M1)$ transition rate is 5 orders of magnitude larger than the basic HFQ M1 $2^1S_0 \rightarrow 1^1S_0 + \gamma(M1)$ transition rate and both transitions are not distinguishable due to their almost equal frequencies.

In Eu^{61+}, the situation is different. The weak asymmetry effect is smaller, but the

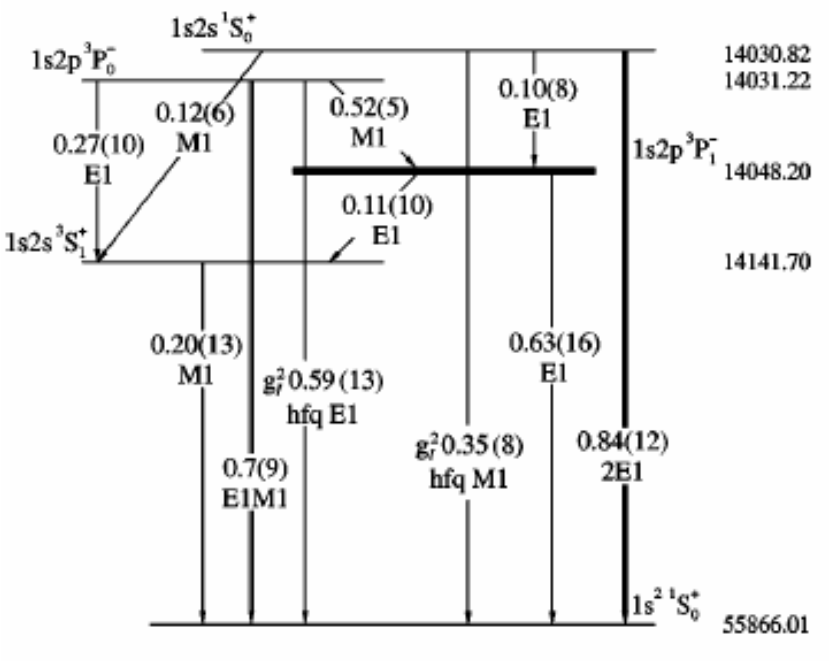

Figure 1: Energy level scheme of the first excited states of heliumlike europium. Numbers on the right-hand side indicate the ionization energies in eV. The partial probabilities of radiative transitions are given in s^{-1}. Numbers in parentheses indicate powers of 10. The large radiative width of the 1s2p $^3P_1$ state is indicated as a bold line. The double lines denote two-photon transitions.

2^1S_0 level lives significantly longer than the 2^3P_0 level. The 2^1S_0 lifetime equals about 1.19 ps and corresponds to a typical decay length of about 0.1 mm in the laboratory. This enables one to "burn off" the 2^3P_0 level and to get rid of the parasitic $2^3P_0 \rightarrow 1^1S_0 + \gamma$ transitions.

2 Production of ion beam polarization: selective laser excitation of hyperfine sublevels

2.1 Polarization of one- and two-electron ions

The polarization of He-like ions in states with the total electron angular momentum equal to zero ($2^1S_0, 2^3P_0$) is actually nuclear polarization.
Due to the relatively strong hyperfine interaction (the HF splitting is of the order of 1 eV for Z $\geq$ 50), the nuclei in one-electron ions with polarized electrons will be polarized within 10^{-15} s. This follows from the energy-time Heisenberg uncertainty relation

$$\Delta E \Delta t \geq \hbar \tag{10}$$

The capture of a second electron into the states $2^1S_0, 2^3P_0$ will not destroy the nuclear polarization, since it occurs via the Coulomb interaction between the electron and the nucleus. Hence, the capture process is much faster than the HF interaction between the second electron and the nucleus.
The amplitude of the destruction process is of the order $(\frac{V_{HFS}}{V_{Coul}})$, where V_{HFS} is the hyperfine interaction and V_{Coul} is the Coulomb interaction between the electron and the nucleus. Then the probability for destruction is of the order $(\frac{V_{HFS}}{V_{Coul}})^2$. Assuming $V_{HFS} \simeq 1eV$ and $V_{Coul} \simeq 60$ keV (binding energy for Z $\simeq$ 63), we obtain

$$\left(\frac{V_{HFS}}{V_{Coul}}\right)^2 \sim 3 \cdot 10^{-10} \tag{11}$$

Thus, the probability of the nuclear polarization destruction during the capture process of the second electron is fully negligible.
Since the direct polarization of the nuclei seems to be a more difficult problem, we come to the idea of producing the polarization first in one-electron ions and then obtain nuclear-polarized He-like ions in the states $2^1S_0, 2^3P_0$ via the capture of a second electron, for example in an appropriate capture foil. In the subsequent sections we will discuss the problems of production and preservation of the polarization of one-electron ion beams in storage rings.

2.2 Radiative polarization: simple estimates

Radiative polarization of electrons arises via radiative transitions between Zeeman sublevels (spin-flip transitions) in an external magnetic field. This was predicted in [28] and realized in practice in Novosibirsk [29].
The transition rate for a spin-flip transition in the rest frame of a particle with spin s = 1/2 is:

$$W_{\uparrow\downarrow} = \frac{4}{3\hbar c^3} | <\uparrow |\vec{\mu}| \downarrow> |^2 w^3 = \frac{64}{3\hbar^4 c^3} \mu_0^5 H^3 \tag{12}$$

where $<\uparrow |\vec{\mu}| \downarrow>$ is the spin-flip matrix element, $\vec{\mu}$ the magnetic moment operator, w the transition frequency, μ_0 Bohr's magneton, and H the external magnetic field. In the laboratory system

$$W_{\uparrow\downarrow} = \frac{64}{3\hbar^4 c^3} |\mu_0|^5 H^3 \gamma^5 \tag{13}$$

where γ is the relativistic enhancement factor

$$\gamma = \left(1 - \frac{v^2}{c^2}\right)^{-1/2} \tag{14}$$

with the particle velocity v. The polarization time is $T_p = W_{\uparrow\downarrow}^{-1}$. For the electrons in the Novosibirsk experiments the parameters in Eq. (13) were: H = 1 T, $\gamma = 10^5$. Then the polarization time was about $T_p \simeq 1$ h.

However, it is impossible to use the same method for heavier particles like protons or bare heavy ions. For protons, the magnetic moment is small and the polarization time becomes huge: $T_p \sim 10^{20}$ h even with the same relativistic enhancement factor.

In principle, the spin-flip mechanism could work for the polarization of H-like heavy ions, since they possess a large magnetic moment of the order of μ_0 (the magnetic moment of an electron). Still, even for the future GSI storage ring with the parameters H = 6T, $\gamma = 23$ [2] one obtains a polarization time $T_p \simeq 10^3$ h, which is too long.

Looking at Eq. (12) one can see that there is a way to enhance the spin-flip probability for highly charged ions. Unlike the elementary particles (electrons, protons), HCI possess excited states and, depending on the nuclear spin, also a hyperfine structure, and one can use transitions between the Zeeman sublevels of the excited and ground hyperfine states, thus greatly enlarging the value of transition frequency ω. This idea was introduced in [30].

2.3 Selective laser excitation of the hyperfine sublevels

In [30] the idea of selective laser excitation of the hyperfine sublevels of the H-like $^{151}_{63}Eu$ ion with a nuclear spin I = 5/2 and the electronic ground state hyperfine sublevels with F = 2 and F' = 3 (F is the total angular momentum of the ion) was exploited. The schematic picture of the ground and excited hyperfine levels for the ground electronic state $1s_{1/2}$ in an external magnetic field is shown in Fig. 2.

The solid vertical lines denote the absorption transitions and the dashed lines show the decay channels for the different Zeeman sublevels. The $1s_{1/2}$ F' = 3 state is excited by a laser with the frequency $w = \Delta E_{hfs} + 2\mu_0 H$, where $\Delta E_{hfs} = 1.513(4)$ eV is the hyperfine splitting [31] and $2\mu_0 H$ is the Zeeman splitting in the external magnetic field. For the experimental scheme proposed in [30] it is not necessary to resolve the Zeeman structure.

The transition probability between the hyperfine sublevels are essentially of M1 type and are given by the expression

$$W(F'M'_F \to FM_F) = A_F \begin{pmatrix} F' & F & 1 \\ \bar{M}'_F & M_F & M'_F - M_F \end{pmatrix}^2 \tag{15}$$

where the standard notation for the 3j-symbol is used, $\bar{M}_F \equiv -M_F$ and the constant A_F is independent of M_F and M'_F.

The selective excitation of the $1s_{1/2}$ F' = 3 magnetic sublevels leads to the polarization of the $1s_{1/2}$ F' = 3 state. The decay of the excited sublevels to the $1s_{1/2}$ F = 2 ground state with the selection rule $M'_F - M_F = 0, \pm 1$ polarizes also the ground state. The population of the magnetic sublevels of the F = 2 state is shifted towards increasing values of M_F: this is the radiative polarization. An evaluation of the M1 $1s_{1/2}F' = 3 \to 1s_{1/2}F = 2$ transition rate according to Eq. (15) yields a lifetime of 10.9 ms for the excited F' = 3 level. Thus, the equilibrium polarization for one

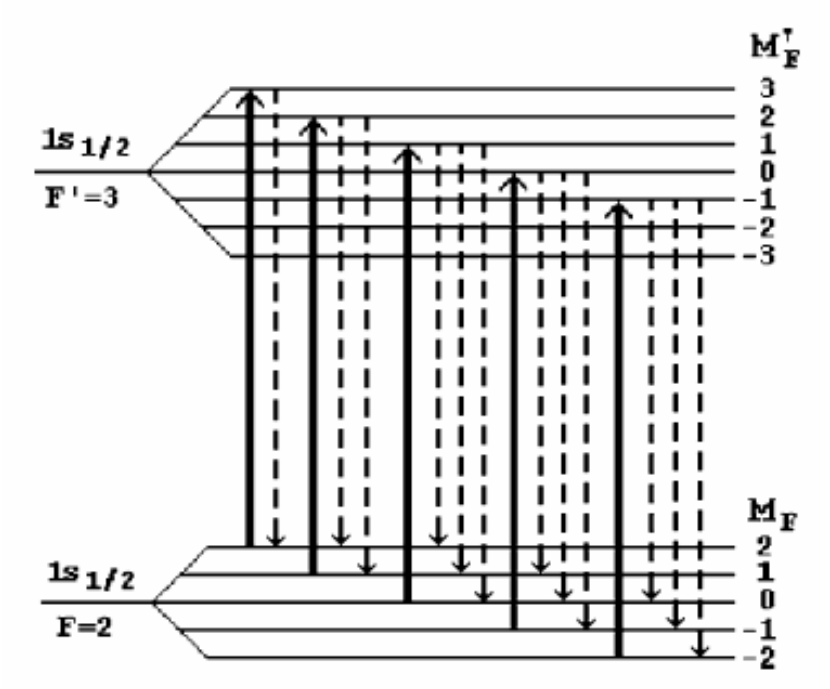

Figure 2: Schematic picture of the Zeeman splitting of the hyperfine sublevels of the ground electronic state for a hydrogenlike $^{151}_{63}$Eu ion. The solid vertical lines denote M1 transitions at the laser frequency $\omega = \Delta E_{hfs} + 2\mu_0 H$. The dashed lines show the decay channels for the different Zeeman sublevels.

laser shot is achieved after 10.9 ms, then the process of laser excitation should be repeated.
In [32, 33] resonant laser excitation measurements of the HFS in H-like $^{207}_{82}Pb$ and $^{209}_{83}Bi$ of ions were performed. It follows from the results of these measurements that during one laser pulse ($\sim$ 50 ns) an equilibrium between the excited and the ground hyperfine levels is established and the occupation numbers for the ground and excited states are equal. In [30] a scenario similar to the one used in [32, 33] was assumed: a laser beam with the proper wavelength is travelling parallel to the ion beam.

2.4 Description of the polarization

The spin-polarized state of an ion is described by the density matrix

$$\rho_F = \sum_{M_F} n_{FM_F} \psi^*_{FM_F} \psi_{FM_F} \tag{16}$$

with the normalization condition

$$\sum_{M_F} n_{FM_F} = 1 \tag{17}$$

where n_{FM_F} are the occupation numbers. We define the degree of polarization as

$$\lambda_F = \frac{1}{F} \sum_{M_F} n_{FM_F} M_F \tag{18}$$

For nonpolarized ions, the distribution of the occupation numbers is uniform $n_{FM_F} = \frac{1}{2F+1}$ and $\lambda_F = 0$. In the case of full polarization $n_{FF} = 1$ and $\lambda = 1$. For the full opposite polarization, $n_{F,-F} = 1$ and $\lambda = -1$.

2.5 The dynamics of the polarization

Each laser shot and the time afterwards until the next shot will be denoted as "cycle". Then the population (occupation) numbers for the excited sublevels $n^{(i)}_{F'M'_F}$ in the i-th cycle under equilibrium conditions are

$$n^{(i)}_{F'M'_F} = \frac{1}{2} n^{(i-1)}_{FM_F} \delta_{M'_F M_{F+1}} \tag{19}$$

where $n^{(i-1)}_{FM_F}$ are the population numbers of the sublevels of the groundstate in the (i-1)the cycle (see Fig. 2). The initial distribution $n^{(0)}_{FM_F}$ is determined by the conditions of the beam preparation; however, it turns out that the final result depends very weakly on these conditions.
The population of the groundstate magnetic sublevels in the ith cycle will be

$$n^{(i)}_{FM_F} = \sum_{M'_F = M_F, M_F \pm 1} \frac{W(F'M'_F \to FM_F)}{\Gamma(F'M'_F)} n^{(i)}_{F'M'_F} \tag{20}$$

where $W(F'M'_F \to FM_F)$ is defined by Eq. (15) and

$$\Gamma(F'M'_F) = \sum_{M_F} W(F'M'_F \to FM_F) \tag{21}$$

is the total width of the excited sublevel $F'M'_F$.
Inserting the expression for $W(F'M'_F \to FM_F)$ from Eq. (15) and using Eq. (19) we obtain a recurrence relations between $n^{(i)}_{FM_F}$ and $n^{(i-1)}_{FM_F}$ which can be used for numerical evaluations. These evaluations give the following results: with the uniform initial population $n^{(0)}_{FM_F} = const$ the first cycle gives $\lambda^{(1)}_F = 0.1667$. After 40 cycles the polarization becomes $\lambda^{(40)}_F = 0.9993$. Actually, one obtains the same result for the case of the opposite initial polarization $n^{(0)}_{F,-F} = -1$. Then $\lambda^{(1)}_F = -0.6667$ and $\lambda^{(40)}_F = 0.9986$. Thus, the building-up time for a degree of polarization at the $\lambda = 0.999$ level equals the time of 40 cycles and $T_p \simeq 0.44$ s. Choosing the alternative selective excitation with frequency $\omega = \Delta E_{HFS} - 2\mu_0 H$, a negative polarization would be obtained within the same time interval.
Unlike the situation in [32, 33] we assume that the magnetic field is oriented longitudinally (along the beam direction). Then, since the quantization axis for the laser photons is parallel to the ion beam and hence to the magnetic field, one can use circularly polarized light for the excitation of the transitions shown in Fig. 2 without resolving the Zeeman structure.

2.6 Nuclear polarization

We define the nuclear polarization density matrix as the density matrix of a subsystem

$$\rho_I = < \psi_{FM_F} | \rho_F | \psi_{FM_F} >_{el} \tag{22}$$

by integration over the electron variables.
The wave function ψ_{FM_F} is expressed by the Clebsch-Gordan expansion

$$\psi_{FM_F} = \sum_{M_I M_J} C^{IJ}_{FM_F}(M_I M_J)\psi_{IM_I}\psi_{JM_J} \tag{23}$$

where ψ_{IM_I} is the nuclear wave function, ψ_{JM_J} is the electron wave function, and $C^{IJ}_{FM_F}(M_I M_J)$ are the Clebsch-Gordan coefficients. The integration in Eq. (22) yields

$$\rho_I = \sum_{M_I} n_{IM_I}\psi^*_{IM_I}\psi_{IM_I} \tag{24}$$

with

$$n_{IM_I} = \sum_{M_J M_F} n_{FM_F}(C^{IJ}_{FM_F}(M_I M_J))^2 \tag{25}$$

We define the degree of the nuclear polarization similar to Eq. (18) as

$$\lambda_I = \frac{1}{I}\sum_{M_I} n_{IM_I} M_I \tag{26}$$

In case of full electron polarization ($n_{FF} = 1$) Eq. (25) results in

$$n_{IM_I} = \sum_{M_J}(C^{IJ}_{FF}(M_I M_J))^2 \tag{27}$$

For H-like $^{151}_{63}$Eu ions in the ground hyperfine state with F = 2 only two possibilities are left regarding the condition $M_F = M_I + M_J = 2$, namely $M_I = 5/2, M_J = -1/2$ and $M_1 = 3/2$, $M_J = 1/2$. Inserting these values into Eq. (27) and evaluating the Clebsch-Gordan coefficients, we obtain $n_{\frac{5}{2}\frac{5}{2}} = \frac{5}{6}$, $n_{\frac{5}{2}\frac{3}{2}} = \frac{1}{6}$. With these occupation numbers the maximum possible value of the nuclear degree of polarization according to Eq. (26) appears to be $\lambda_I^{max} = 0.93$.

3 Diagnostics of the ion spin-polarization

3.1 Radiative electron capture as a probe process

The spin polarization of heavy ions in storage rings by optical pumping or any another technique is of little help for future studies if the degree of ion polarization λ_F cannot be controlled experimentally. For such a control, it is necessary to find a physical process which is sensitive enough to the spin states of high-Z ions and which can be measured easily and online. Based on the detailed theoretical analysis, we have recently suggested to employ *radiative capture* of a free (or quasi-free) electron by the projectile as a "probe" process [34]. The radiative electron capture (REC), which is the time-reversed photoeffect and hence is accompanied by the emission of photons, is *efficient* as it is the dominant process in relativistic collisions of high-Z projectiles with electronic and atomic targets.

In the past, the REC of highly-charged ions has been explored in great details in a number of experiments [35, 36, 37]. For example, by making use of recent advances in the design of x-ray detection techniques, first measurements of the linear polarization of the recombination photons have been performed for the capture of an electron into the K-shell of bare uranium ions [38]. When compared with theory, such polarization measurements are quantitatively well described by means of the density matrix formalism, based on Dirac's relativistic equation [39, 40]. Apart from the explanation of the available experimental data, the density matrix treatment of the REC also predicts that the linear polarization of the emitted photons is strongly influenced by the spin-polarization of the (incident) ions [34]. Such a *polarization transfer*, therefore, opens a way for determining the spin properties of the ion beam.

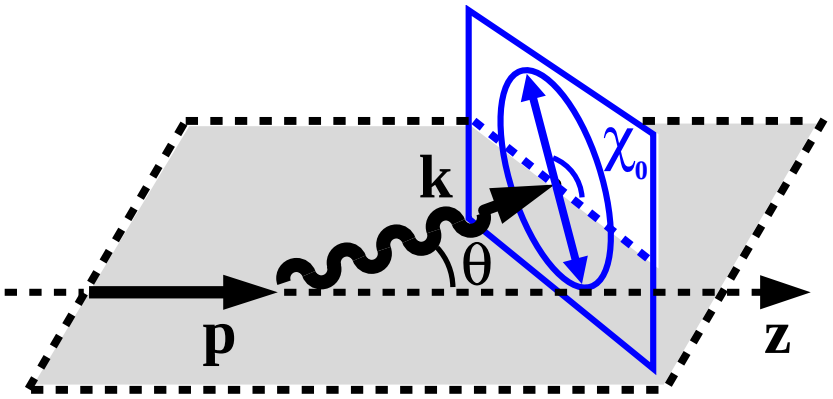

Figure 3: Definition of the polarization ellipse; its principal axis is characterized by the angle χ_0 with respect to the reaction plane which is formed by the directions of incoming ion beam and emitted photons.

3.2 The Stokes parameters and the polarization ellipse of the emitted photons

In order to understand how the polarization transfer in the radiative electron capture may help with the diagnostics of the ion spin-polarization, we have first to agree how the polarization for both the incoming hydrogen-like ions and the emitted x-ray photons is described. While the spin states of ion polarization is characterized by an (averaged) parameter defined in Eq. (18), the polarization of the recombination photons is described most conveniently in terms of the *Stokes parameters*. These parameters are determined by the intensity if I_χ of the linear polarized light measured at different angles χ with respect to the reaction plane which is as formed by the directions of the incident ion beam and the emitted photons. While the first Stokes parameter

$$P_1 = \frac{I_0 - I_{90}}{I_0 + I_{90}} \tag{28}$$

is derived from the intensities *parallel* and *perpendicular* to the reaction plane, the parameter P_2 follows from a similar ratio, taken at $\chi = 45^\circ$ and $\chi = 135^\circ$, respectively:

$$P_2 = \frac{I_{45} - I_{135}}{I_{45} + I_{135}} \tag{29}$$

The Stokes parameters are very convenient not only for an experimental but also for a theoretical analysis of the light polarization since they are directly related to the photon spin-density matrix in the *helicity* representation:

$$\left\langle \mathbf{k}\lambda \left| \hat{\rho}_\gamma \right| \mathbf{k}\lambda' \right\rangle = \frac{1}{2} \begin{pmatrix} 1 + P_3 & P_1 - iP_2 \\ P_1 + iP_2 & 1 - P_3 \end{pmatrix}, \tag{30}$$

where $\mathbf{k}$ denotes the wave vector and $\lambda = \pm 1$ the helicity of the recombination photons, that is their spin projection onto the direction of propagation. A third Stokes parameter P_3, finally, reflects the degree of the circular polarization of the light.

The two Stokes parameters P_1 and P_2 specify the linear polarization of the radiation completely, i.e., both the degree of the polarization as well as its direction in the plane perpendicular to the photon momentum $\mathbf{k}$. Instead of the Stokes parameters, however, we may represent the linear polarization of the emitted x rays also in

terms of a *polarization ellipse* which is defined in the plane perpendicular to **k**. This ellipse is characterized by the relative length $P_L = \sqrt{P_1^2 + P_2^2}$ of the principal axis as well as the angle χ_0 with respect to the reaction plane [cf. Figure 3]. When expressed in terms of the Stokes parameters, this angle is given by the ratio

$$\tan 2\chi_0 = \frac{P_2}{P_1} \tag{31}$$

and thus can be used as a single parameter for analyzing the direction of the polarization of the emitted light. In the next subsection we will show how the angle χ_0 of the polarization ellipse of recombination photons is related to the spin states of the incoming hydrogen-like ions.

3.3 The polarization transfer in electron capture

We are now prepared to study the influence of an initially polarized ion beam on the Stokes parameters and, thereby, on the polarization ellipse of the emitted recombination photons. In order to start such a polarization analysis, we note that the Stokes parameters can be expressed in terms of the (matrix) elements of the photon spin-density matrix given by Eq. (30). For the radiative capture of a free unpolarized electron with asymptotic momentum **p** and spin projections $m_s = \pm 1/2$ into the hyperfine bound state $\left|\tilde{F}\tilde{M}_F\right\rangle$ of the subsequently helium-like projectile, the matrix elements are obtained by standard techniques [34]

$$\begin{aligned} \left\langle \mathbf{k}\lambda \,|\, \hat{\rho}_\gamma \,|\, \mathbf{k}\lambda' \right\rangle &= \frac{1}{2} \sum_{M_F m_s} \sum_{\tilde{F}\tilde{M}_F} M^*_{\mathbf{p}}(m_s, M_F; \lambda, \tilde{F}, \tilde{M}_F) \\ &\times \; M_{\mathbf{p}}(m_s, M_F; \lambda', \tilde{F}, \tilde{M}_F)\, n_{FM_F} \end{aligned} \tag{32}$$

They indicate that the spin state of the emitted photons depends both on the amplitudes $M_{\mathbf{p}}(m_s, M_F; \lambda, \tilde{F}, \tilde{M}_F)$ for the capture of the electron *as well as* on the (relative) population n_{FM_F} of the hyperfine sublevels $|FM_F\rangle$ of the initially hydrogen-like ions.

Inserting the spin-density matrix (32) into Eq. (30), we are able to express the Stokes parameters for the recombination photons in terms of the (reduced) transition matrix elements. For the sake of brevity, we omit here the details of this derivation and just discuss the final results which predict for the K-shell electron capture that the two Stokes parameters P_1 and P_2 behave in rather different ways with respect to the spin-polarization of hydrogen-like projectile ions. While the parameter P_1 does not depend on beam polarization and, hence, can not be used for polarization studies, the second Stokes parameter P_2 appears to be proportional to the degree of the beam polarization defined in Eq. (18):

$$P_2 \;\sim\; \lambda_F = \frac{1}{F} \sum_{M_F} n_{FM_F} M_F \tag{33}$$

The Stokes parameter P_2 may serve, therefore, as a valuable tool for measuring the polarization properties of the heavy ion beams at storage rings.

Instead of analyzing a single parameter P_2, it is even more convenient to study the overall *rotation* of the linear polarization of the recombination photons out of the reaction plane. As discussed already, such a rotation is characterized by the angle χ_0. For the electron recombination into the K-shell of polarized hydrogen-like ions this angle can be obtained from Eqs. (31) and (33):

$$\tan 2\chi_0 \sim \lambda_F \tag{34}$$

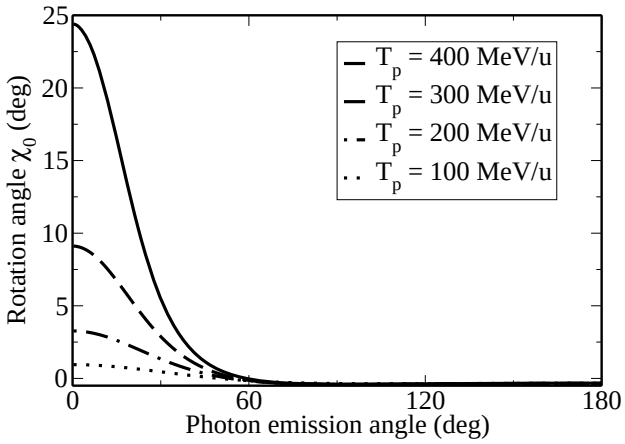

Figure 4: Rotation angle χ_0 of the polarization ellipse of the emitted photons following the capture of unpolarized electrons into the K-shell of hydrogen-like europium ions (with nuclear spin $I = 5/2$). Calculations are presented for completely polarized projectile ions ($\lambda_F = 1$) and in the laboratory frame.

As can be seen from Eq. (34), the capture of electrons by unpolarized hydrogen-like ions, $\lambda_F = 0$, always leads to an emission of light which is polarized either within or perpendicular to the reaction plane ($\chi_0 = 0^\circ$ or $\chi_0 = 90^\circ$), while any contribution from a nonzero λ_F parameter will rotate the polarization ellipse ($\chi_0 \neq 0^\circ$ and $\chi_0 \neq 90^\circ$) out of the reaction plane. The measurement of the rotation angle χ_0 therefore provide a direct access to the degree λ_F of the polarization of the incoming ions without a detailed analysis of the Stokes parameters or the shape of the polarization ellipse needs to be analyzed in detail.
Figure 4 displays the rotation angle χ_0 as calculated, for example, for radiative capture of electrons into the ground state of completely polarized ($\lambda_F = 1$) hydrogen-like europium ions with energies in the range 100 MeV/u $\leq$ Tp $\leq$ 400 MeV/u. As can be seen from this figure, the effect of the ion polarization becomes particularly remarkable for the forward emission of the recombination photons. Note, however, that χ_0 is not defined at the emission angle $\theta = 0^\circ$ (or $\theta = 180^\circ$), because photon emission in either the forward or backward direction does not break the axial symmetry for the collision system. For the angle $\theta = 0^\circ$, therefore, the linear polarization of the light must always be zero. At larger angles of, say $10^\circ < \theta < 60^\circ$, however, the degree of linear polarization becomes large enough for experiments and preferable for first investigations of the polarization of ion beams.

4 Preservation of the polarization in storage rings

4.1 Depolarization mechanisms

One of the possible depolarization mechanisms of polarized ion beams in storage rings is the influence of the quickly changing fields when the ions meet the magnetic system of the ring. In principle, shake-off processes could occur, which would destroy the polarization. These effects are absent in the classical field limit, when the nonstationary Schrödinger equation is applied for the description of the spin motion

in a time-dependent magnetic field. This equation describes the spin behavior in the rest-frame of a particle moving in a storage ring. If this equation has a well-defined solution, the shake-off processes are absent. The criteria for the existence of such a solution are the standard mathematical criteria of the "smoothness" of the field functions, the absence of discontinuities etc.
Physically, these criteria are fulfilled for example by the exponentially dropping fringe fields of the bending magnets in the GSI storage ring ESR.
Another possible depolarization mechanism relates to spin resonances. The polarization of the ion beam can be destroyed by any external periodic force if the period of this force coincides with the period of the spin precession of a polarized state. In a storage ring, the role of this external periodic force can be played by the Lorentz force which enables the revolution of a particle around the ring. If the revolution frequency coincides with the Larmor frequency of the spin precession (or with one of its lower harmonics), a spin resonance can occur.
Spin resonances are unavoidable when the particles are accelerated (like electrons in a synchrotron) but can be avoided when the particles have a fixed energy, like ions in a storage ring.
Therefore, we will neglect both mechanisms of depolarization. However, even in the absence of these mechanisms the preservation of the polarization of the ion beam in the storage ring remains to be a severe problem. In the following we treat this problem applying the procedure adopted in Ref. [41]

4.2 Instantaneous quantization axis

Aiming for a quantum-mechanical description of the motion of a hydrogen-like heavy ion in a magnetic field, we consider the dynamics of a particle with total angular momentum $\vec{s}$, which will be called in the following as spin. For nuclei with nonzero nuclear spin I, s = I $\pm$ 1/2 = F with m_s = -s, ..., +s. Since this investigation is oriented at the presently existing ion storage rings like the ESR with the relativistic factor $\gamma \approx 1$, we need neither the relativistic wave equation nor the Bargmann-Michel-Telegdi equation [42] for the description of the spin motion.
The Schrödinger equation for the spin wave function $\chi_s(t)$ reads

$$\left[i\hbar\frac{\partial}{\partial t} + \mu\vec{\mathcal{H}}(t)\cdot\vec{s}\right]\chi_s(t) = \left[i\hbar\frac{\partial}{\partial t} + \mu\cdot\hat{s}_{\mathcal{H}}(t)\right]\chi_s(t) = 0 \tag{35}$$

where $\vec{s}$ is the spin operator, $\hat{s}_{\mathcal{H}}(t) = \vec{s}\vec{\mathcal{H}}$, μ is the magnetic moment of the bound electron of the order $2\mu_0$, where $\mu_0 = \frac{e\hbar}{2mc}$ is the Bohr magneton, $\hbar$ is the Planck constant, e, m are the electron charge and mass, c is the speed of the light and $\vec{\mathcal{H}}(t)$ is the time-dependent magnetic field experienced by the ions in their rest frame.
We introduce the time-dependent instantaneous quantization axis (IQA) $\vec{\gamma}$ with respect to which the degree of polarization remains constant. The existence of the IQA is actually equivalent to the existence of a definite polarization. The IQA presents also a convenient tool for the investigation of depolarization effects.
To prove the existance of the IQA we introduce first the spin projection operator onto the IQA

$$\hat{s}_\gamma(t) = \hat{\vec{s}}\vec{\gamma} \tag{36}$$

This operator is Hermitian, and at a given time moment it possesses a complete set of eigenfunctions in the spin space with real eigenvalues obtained from the solution of

$$\hat{s}_\gamma(t)\chi_{sm_s}(t) = m_s\chi_{sm_s}(t) \tag{37}$$

The arbitrary solution of the nonstationary equation can be expanded in the complete set $\chi_{sm_s}(t)$

$$\chi_s(t) = \sum_{m_s} a_{sm_s}(t)\chi_{sm_s}(t) \tag{38}$$

The IQA is defined by the equation

$$\frac{\partial}{\partial t} < \chi_s(t)|\hat{s}_\gamma(t)|\chi_s(t) >= 0 \tag{39}$$

Using Eq. (35) for the differentiation yields

$$\frac{\partial}{\partial t} < \chi_s(t)|\hat{s}_\gamma(t)|\chi_s(t) >=< \chi_s(t)|i\frac{\mu}{\hbar}\left[\mathcal{H}_k(t)\hat{s}_k\hat{s}_i\gamma_i(t) - \hat{s}_i\gamma_i(t)\mathcal{H}_k\hat{s}_k\right] + \hat{s}_i\frac{\partial\gamma_i}{\partial t}|\chi_s(t) >$$

where we adopted Einstein's rule for summation over repeating indices. With the help of the commutation relation

$$\hat{s}_i\hat{s}_k - \hat{s}_k\hat{s}_i = i\varepsilon_{ikl}\hat{s}_l \tag{40}$$

where ε_{ikl} is the fully antisymmetric unit tensor and the definition of the vector product

$$(\vec{a}\times\vec{b})_l = \varepsilon_{ikl}a_ib_k \tag{41}$$

we arrive at the equality

$$\frac{\partial}{\partial t} < \chi_s(t)|\hat{s}_\gamma(t)|\chi_s(t) >=< \chi_s(t)|\left[\frac{\partial\vec{\gamma}(t)}{\partial t} - \frac{\mu}{\hbar}\left(\vec{\mathcal{H}}(t)\times\vec{\gamma}(t)\right)\right]\hat{\vec{s}}|\chi_s(t) > \tag{42}$$

Then Eq. (39) is fulfilled if the IQA satisfies the equation

$$\frac{\partial\vec{\gamma}(t)}{\partial t} = \frac{\mu}{\hbar}(\vec{\mathcal{H}}(t)\times\vec{\gamma}(t)) \tag{43}$$

In principle, the solution of Eq. (43) with the given initial condition should exist for any physically reasonable function $\vec{\mathcal{H}}(t)$. This proves the existence of the IQA. Eq. (43) coincides with the equation for the classical angular momentum motion. In this sense the existence of a IQA means simply the existence of polarization and the direction of the polarization coincides always with the direction of the IQA. However, for our purposes we need to prove the more delicate statement of the constancy of the degree of polarization with respect to the IQA. This is not a classical but a quantum-mechanical property. As far as we know this statement has never been proved before.
Insertion of the expansion Eq. (38) into Eq. (39) results in

$$\frac{\partial}{\partial t}\sum_{m_s}|a_{sm_s}(t)|^2m_s = 0 \tag{44}$$

The matrix elements in Eq. (39) can be presented also in another way via the spin density matrix. We employ the spin density matrix from [30]

$$\rho_s(t) = \sum_{m_s} n_{sm_s}(t)\chi^*_{sm_s}(t)\chi_{sm_s}(t) \tag{45}$$

where $n_{sm_s}(t)$ are the occupation numbers with respect to the IQA. These occupation numbers $n_{sm_s}(t)$ are connected to the amplitudes $a_{sm_s}(t)$ via

$$n_{sm_s}(t) = |a_{sm_s}(t)|^2 \tag{46}$$

Then

$$< \chi_s(t)|\hat{s}_\gamma(t)|\chi_s(t) >= Tr(\rho_s(t)\hat{s}_\gamma(t)) = \sum_{m_s} m_s n_{sm_s}(t) \tag{47}$$

From the definition of the degree of polarization λ_s ([30])

$$\lambda_s = \frac{1}{s}\sum_{m_s} m_s n_{sm_s}(t) \tag{48}$$

we find from Eq. (48) and Eq. (39)

$$\lambda_s = \frac{1}{s}\sum_{m_s} m_s n_{sm_s}(t) = \frac{1}{s} < \chi_s(t)|\hat{s}_\gamma(t)|\chi_s(t) >= const \tag{49}$$

We note that only the degree of polarization λ_s remains constant, while the occupation numbers of the magnetic sublevels $n_{sm_s}(t)$ have a general time dependence.

4.3 Conservation of the polarization in the spontaneous decay process

The mechanism of polarization proposed in [30] implies a selective laser excitation of hyperfine levels and a spontaneous decay from the excited hyperfine levels to the ground state. The fact that only the degree of polarization λ_s, but not the occupation numbers of the magnetic sublevels $n_{sm_s}(t)$ remains constant necessitates to prove the conservation of the degree of polarization in the spontaneous decay process.

It has been argued in Ref. [30] that the connection between the occupation numbers $n_{s+1m_{s+1}}$ of the magnetic sublevels of the excited hyperfine level and the occupation numbers n_{sm_s} of the magnetic sublevels of the ground hyperfine level in process of spontaneous decay is given by (cf. Eq. (20)).

$$n_{sm_s} = \sum_{m_{s+1}} \frac{W(s+1, m_{s+1} \to s, m_s)}{\Gamma_{s+1,m_{s+1}}} n_{s+1m_{s+1}} \tag{50}$$

where $W(s+1, m_{s+1} \to s, m_s)$ is the probability of the M1-transition between the $(s+1, m_{s+1})$ and (s, m_s) magnetic sublevels of the excited and ground hyperfine levels and $\Gamma_{s+1,m_{s+1}}$ is the width of the excited sublevel (cf. Eq. (21)).

$$\Gamma_{s+1,m_{s+1}} = \sum_{m_s} W(s+1, m_{s+1} \to s, m_s) \tag{51}$$

According to Ref. [30]

$$W(s+1, m_{s+1} \to s, m_s) = A \begin{pmatrix} s+1 & s & 1 \\ -m_{s+1} & m_s & m_{s+1}-m_s \end{pmatrix}^2 \tag{52}$$

where A is a constant. Then using the expressions for the 3j-symbols (see [43])

$$\begin{pmatrix} s+1 & s & 1 \\ -m_{s+1} & m_{s+1} & 0 \end{pmatrix}^2 = \frac{2(s+1+m_{s+1})(s+1-m_{s+1})}{(2s+1)(2s+2)(2s+3)} \tag{53}$$

$$\begin{pmatrix} s+1 & s & 1 \\ -m_{s+1} & m_{s+1}-1 & 1 \end{pmatrix}^2 = \frac{(s+m_{s+1})(s+1+m_{s+1})}{(2s+1)(2s+2)(2s+3)} \tag{54}$$

$$\begin{pmatrix} s+1 & s & 1 \\ -m_{s+1} & m_{s+1}+1 & -1 \end{pmatrix}^2 = \frac{(s-m_{s+1})(s+1-m_{s+1})}{(2s+1)(2s+2)(2s+3)} \tag{55}$$

the width is given by

$$\Gamma_{s+1,m_{s+1}} = \sum_{m_s} W(s+1, m_{s+1} \to s, m_s) = \sum_{m_s} A \bullet \begin{pmatrix} s+1 & s & 1 \\ -m_{s+1} & m_s & m_{s+1}-m_s \end{pmatrix}^2 = \frac{A}{2s+3} \tag{56}$$

Thus, the magnetic sublevel widths for the excited hyperfine level are all equal to each other.
To prove the conservation of polarization in the process of spontaneous decay we insert Eq. (51) into Eq. (49) and change the order of summation

$$\lambda_s = \frac{1}{s}\sum_{m_s} m_s n_{sm_s} = \frac{1}{s}\sum_{m_s} m_s \sum_{m_{s+1}} \frac{W(s+1, m_{s+1} \to s, m_s)}{\Gamma_{s+1,m_{s+1}}} n_{s+1m_{s+1}} = \frac{1}{s}\sum_{m_{s+1}} n_{s+1m_{s+1}} \sum_{m_s} m_s \frac{W(s+1, m_{s+1} \to s, m_s)}{\Gamma_{s+1,m_{s+1}}} = \frac{1}{s}\sum_{m_{s+1}} n_{s+1m_{s+1}} C_{m_{s+1}} \tag{57}$$

Direct evaluation of the coefficient $C_{m_{s+1}}$ using Eqs. (53)-(56) yields

$$C_{m_{s+1}} = \sum_{m_s} m_s \frac{W(s+1, m_{s+1} \to s, m_s)}{\Gamma_{s+1,m_{s+1}}} = (2s+3)\sum_{m_s} m_s \bullet \begin{pmatrix} s+1 & s & 1 \\ -m_{s+1} & m_s & m_{s+1}-m_s \end{pmatrix}^2 = m_{s+1}\frac{s}{s+1} \tag{58}$$

Inserting the result of Eq. (58) into Eq. (57) one obtains:

$$\lambda_s = \frac{1}{s+1}\sum_{m_{s+1}} n_{s+1m_{s+1}} m_{s+1} = \lambda_{s+1} \tag{59}$$

This equivalence proves that the degree of polarization is conserved in the process of spontaneous decay.

4.4 Rotation of the IQA in the magnetic system of a storage ring

In case of the radiative polarization of the ion beam it was assumed in [30] that the polarization occurs via selective laser excitation of certain magnetic sublevels of the hyperfine levels of an ion in a longitudinal magnetic field. The other possibility, also considered in [30], was to employ for the excitation a circularly polarized laser beam oriented along the ion beam direction in the absence of the magnetic field. In both cases, the radiative decay of the upper excited hyperfine level would lead to the polarization of the lower hyperfine level during the ion's revolutions around the ring. The decay time for the upper hyperfine level is about 10 ms ($Z \geq 50$) and after this time the laser shot should be repeated. The existence of the IQA ensures that the polarization will grow up during the decay time and, in case of $^{151}_{63}$Eu ions will reach the value $\lambda = 0.167$, provided that the initial polarization value was $\lambda = 0$. After approximately 40 shots the polarization becomes close to

100%. This occurs independent of the instantaneous direction of the IQA during the many ion's revolutions around the ring. However, at the moment of the second laser shot the IQA should be oriented again longitudinally.

To study this problem we will consider the solutions of Eq. (43) for a few simple examples. In case of a constant magnetic field $\vec{\mathcal{H}}$ with initial condition $\vec{\gamma}(0) \parallel \vec{\mathcal{H}}$, Eq. (43) has the evident solution $\vec{\gamma} \parallel \vec{\mathcal{H}}$. In particular, $\vec{\gamma}$ coincides with the direction of the longitudinal magnetic field when the polarization arises in the cooler magnet due to the mechanism as described in [30]. In general, for a time-dependent magnetic field $\vec{\mathcal{H}}(t)$ the direction of $\vec{\gamma}(t)$ does not coincide with $\vec{\mathcal{H}}(t)$.

Even for a constant magnetic field but with the initial condition for Eq. (43) different from $\vec{\gamma}(0) \parallel \vec{\mathcal{H}}$, the IQA does not coincide with the direction of $\vec{\mathcal{H}}$. As an example we consider the simplest case of a magnetic field directed along the x (vertical) axis. The initial polarization we assume to be oriented along the z axis which is the direction of the ion velocity. Then the solution of Eq. (43) with magnetic field $\mathcal{H}_x = \mathcal{H}$, $\mathcal{H}_y = \mathcal{H}_z = 0$ and with the initial conditions for the unit vector $\vec{\gamma} = (\gamma_x, \gamma_y, \gamma_z) = (0, 0, 1)$ results in $\gamma_x = 0$, $\gamma_y = \sin\omega t$, $\gamma_z = \cos\omega t$. Thus the IQA rotates in the yz plane, perpendicular to the direction of magnetic field, with the time-independent frequency $\omega = \frac{1}{\hbar}\mu\mathcal{H}$.

In a more general case, when $\mathcal{H}_x = \mathcal{H}(t)$, $\mathcal{H}_y = \mathcal{H}_z = 0$, i.e. when the magnetic field is changing its magnitude but not the direction, the solution of Eq. (43) reads with the same initial conditions $\gamma_x = \gamma_y = 0$, $\gamma_z = 1$

$$\gamma_x = 0 \tag{60}$$

$$\gamma_y = \sin\varphi(t) \tag{61}$$

$$\gamma_z = \cos\varphi(t) \tag{62}$$

$$\varphi(t) = \frac{\mu}{\hbar}\int_0^t \mathcal{H}(t')dt' \tag{63}$$

This corresponds to the real situation where the longitudinally polarized ion (longitudinal direction corresponds to the z axis) meets the magnetic field of a bending magnet. The latter field has a vertical orientation (along the x axis). The IQA again rotates in the yz (horizontal) plane with the time-dependent frequency $\omega(t) = \varphi(t)/t$.

The problem arises since the bending magnet rotates the beam trajectory due to the Lorentz force. The ion velocity changes its direction according to the equation of motion

$$\dot{v} = -\frac{Ze}{Mc}(\vec{\mathcal{H}} \times \vec{v}) \tag{64}$$

where $\vec{v}$ is the ion velocity, Z is the charge of the nucleus, and M is the mass of the nucleus. Roughly we can write the rotation angle α for the ion trajectory as

$$\alpha = \mu_N \int_0^t \mathcal{H}(t')dt' \tag{65}$$

where

$$\mu_N = \frac{2Zm}{M}\frac{\mu_0}{\hbar}. \tag{66}$$

For $^{151}_{63}$Eu ions $\mu_N = 4,54 \cdot 10^{-4}\frac{\mu_0}{\hbar}$.

Comparing Eq. (65) and Eq. (63) we conclude that the rotation angle for the IQA after passing only one bending magnet of 60^0 ($\pi/3$) will be of the order $10^4\pi$. Thus, it will be extremely difficult to fix the direction of the IQA parallel to the ion beam direction at the moment of the next laser shot.

4.5 Further depolarization effects and conclusions

A serious problem arises also due to the velocity spread Δv of the stored ions. The relative velocity spread $\frac{\Delta v}{v}$ leads to a spread $\Delta\varphi \approx \alpha \frac{\Delta v}{v}$ in the rotation angle. Then, with $\frac{\Delta v}{v} \approx 10^{-5}$ and a revolution frequency of 1 MHz which correspond to the conditions in the GSI ring, one obtains an angle-spread $\Delta\varphi \approx 20\pi$ (for $\alpha = \pi/3$) after 1 sec. This actually means the full depolarization of the beam.
The situation can be improved by the use of "Siberian snakes", i.e. of special magnets which rotate the direction of the polarization of particles. These snakes were first used in Novosibirsk [29, 44], for the rotation of the electron polarization, and in the Indiana proton storage ring for the rotation of the proton polarization [45].
In the case of the GSI storage ring, the first rotating snake should be placed in front of the first bending magnet behind the longitudinal polarizing magnet and should rotate the polarization by an angle $\pi/2$ to the vertical direction. Then the IQA will coincide with the direction of the magnetic field of the bending magnet and the latter will not rotate the IQA. Field inhomogenouities in the direction of the bending magnet will produce an uncertainty in the determination of the beam polarization. To achieve an accuracy of the order of 0.5% for PNC experiments with HCI, these inhomogenuities should be kept at a level of 10^{-3}. In front of the longitudinal magnet an another rotating snake should be placed which would rotate the IQA back by an angle $\pi/2$ so that the direction of the polarization will become again longitudinal.
The use of the snakes, however, dos not help to avoid the problem with focussing (quadrupole) magnets and other external magnetic fields, among them the magnetic field of the earth ($\sim 0.5 \times 10^{-4}$ T) and the unknown magnetic fields of various metallic parts of the ring equipment.
Another depolarization factor is the cooling magnet. Due to its longitudinal field, this magnet can be used in principle as a polarization magnet. However, the cooling electrons, co-propagating with one-electron ions in the beam, can produce also depolarization. The most simple solution of the problem would be switching off the electron source for the polarization time (about 0.5 s).
In order to overcome these problems it seems to be unavoidable to build a heavy-ion storage ring which is especially devoted to the preservation of the polarization of highly-charged ions. As a minimum requirement, this ring should be screened from external magnetic fields. Finally, it should be noted that almost all of the polarization-destroying effects are negligibly small, if polarized bare nuclei are injected, stored and accumulated in the ring.

References

[1] F. Bosch and P. Egelhof, Eds. Proc. 3rd Int. Conf. on Nuclear Physics at Storage Rings, Bernkastel-Kues, 1996, Elsevier, Amsterdam 1997

[2] W. Henning, Ed. Conceptual Design Report for an International Accelerator Facility for Beams of Ions and Antiprotons at GSI, 441 (2001)

[3] I.B. Khriplovich, Phys. Lett. B444, 98 (1998); Hyperfine Int. 127, 365 (2000)

[4] K. Jungmann, G.P. Berg, U. Dammalapati, P. Dendooven, O. Dermois, M.N. Harakeh, R. Hoekstra, R. Morgenstern, V. Traykov, L. Willmann, and H.W. Wilschut, Phys. Scr. T104, 178 (2003)

[5] S. Weinberg, Phys. Rev. D5, 1412 (1972)

[6] A. Salam, Proc. of 8th Nobel Symp. (N.Y. Wiley, 1968)

[7] Sh. L. Glashow, Nucl. Phys. 22, 579 (1961)

[8] M.A. Bouchiat and C. Bouchiat, J. Phys. (Paris) 35, 899 (1974); 36, 493 (1974)

[9] I.B. Khriplovich, Sov. Phys. JETP Lett. 20, 315 (1974)

[10] L.M. Barker and M.S. Zolotorev, Sov. Phys. JETP Lett. 27, 357 (1978)

[11] C.S. Wood, S.C. Bennett, D. Cho, B.P. Masterson, J.L. Roberts, C.E. Tanner, and C.E. Wieman, Science 275, 1759 (1997)

[12] S.C. Bennett and C.E. Wieman, Phys. Rev. Lett. 82, 2484 (1999), 83, 889 (1999)

[13] I.B. Khriplovich, Parity Nonconservation in Atomic Phenomena (Gordon and Breach, London, 1991)

[14] J.S.M. Gringes and V.V. Flambaum, Phys. Rep. 397, 63 (2004)

[15] V.V. Flambaum and I.B. Khriplovich, Sov. Phys. JETP 52, 835 (1980)

[16] Ya.B. Zel'dovich, Sov. Phys. JETP 6, 1184 (1958)

[17] A.N. Moskalev, JETP Lett. 19, 216 (1974)

[18] Ya. I. Azimov, A.A. Anselm, A.N. Moskalev, and R.M. Ryndin, Zh. Eurp. Theor. Fiz 67, 17 (1974)

[19] V.G. Gorshkov and L.N. Labzowsky, Pis'ma Zh. Eurp. Theor. Fiz 19, 768 (1974); Sov. Phys. JETP 42, 581 (1975)

[20] A. Schäfer, G. Soff, P. Indelicato, B. Müller, and W. Greiner, Phys. Rev. A40, 7362 (1989)

[21] V.V. Karasiev, L.N. Labzowsky, and A.V. Nefiodov, Phys. Lett. A172, 62 (1992)

[22] R.W. Dunford, Phys. Rev. A54, 3820 (1996)

[23] L.N. Labzowsky, A.V. Nefiodov, G. Plunien, G. Soff, R. Marrus, and D. Liesen, Phys. Rev. A63, 054105 (2001)

[24] A.V. Nefiodov, L.N. Labzowsky, D. Liesen, G. Plunien, and G. Soff, Phys. Lett. B534, 52 (2002)

[25] L. Labzowsky, G. Klimchitskaya, and Yu. Dmitriev, Relativistic Effects in the Spectra of Atomic Systems, IOP Publishing, 1993

[26] V.M. Shabaev, I.I. Tupitsyn, K. Pachucki, G. Plunien, and V.A. Yerokhin, Phys. Rev. A72, 062105 (2005)

[27] A.N. Artemyev, V.M. Shabaev, V.A. Yerokhin, G. Plunien, and G. Soff, Phys. Rev. A71, 062104 (2005)

[28] A.A. Sokolov and I.M. Ternov, Sov. Phys. Dokl. 8, 1203 (1964)

[29] Ya. S. Derbenev, A.M. Kondratenko, S.I. Serednyakov, A.N. Skrinsky, G.M. Tumaikin, and Yu.M. Shatunov, Particle Accelerators 8, 115 (1978)

[30] A. Prozorov, L. Labzowsky, D. Liesen, and F. Bosch, Phys. Lett. B574, 180 (2003)

[31] V.M. Shabaev, M. Tomaselli, T. Kühl, A.N. Artemyev, and V.A. Yerokhin, Phys. Rev. A56, 252 (1997)

[32] I. Klaft, S. Borneis, T. Engel, B. Fricke, R. Griesser, G. Huber, T. Kühl, D. Marx, R. Neumann, S. Schröder, P. Seelig, and L. Völker, Phys. Rev. Lett. 73, 2425 (1994)

[33] P. Seelig, S. Borneis, A. Dax, T. Engel, S. Faber, M. Gerlach, C. Holbrow, G. Huber, T. Kühl, D. Marx, K. Meier, P. Merz, W. Quint, F. Schmitt, M. Tomaselli, L. Völker, H. Winter, M. Würtz, K. Beckert, B. Franzke, F. Nolden, H. Reich, M. Steck, and T. Winkler, Phys. Rev. Lett. 81, 4824 (1998)

[34] A. Surzhykov, S. Fritzsche, Th. Stöhlker and S. Tashenov, Phys. Rev. Lett. 94, 203202 (2005).

[35] Th. Stöhlker, Phys. Scr. T80, 165 (1999).

[36] Th. Stöhlker, D. Banas, S. Fritzsche, A. Gumberidze, C. Kozhuharov, X. Ma, A. Orsic-Muthig, U. Spillmann, D. Sierpowski, A. Surzhykov, S. Tachenov, and A. Warczak, Phys. Scr. T110, 384 (2004).

[37] J. Eichler and Th. Stöhlker, Physics Reports 439, 1 (2007).

[38] S. Tashenov, Th. Stöhlker, D. Banaś, K. Beckert, P. Beller, H. F. Beyer, F. Bosch, S. Fritzsche, A. Gumberidze, S. Hagmann, C. Kozhuharov, T. Krings, D. Liesen, F. Nolden, D. Protic, D. Sierpowski, U. Spillmann, M. Steck, and A. Surzhykov, Phys. Rev. Lett. 97, 223202 (2006).

[39] A. Surzhykov, S. Fritzsche, and Th. Stöhlker, Phys. Lett. A 289, 213 (2001).

[40] J. Eichler and A. Ichihara, Phys. Rev. A 65, 052716 (2002).

[41] A. Prozorov, G. Plunien, L. Labzowsky, D. Liesen, and F. Bosch, On the preservation of the polarizaiton of polarized ion beams in the magnetic system of a storage ring, accept. for publication in Phys. Lett. B

[42] V. Bargmann, L. Michel and V. Telegdi, Phys. Rev. Lett. 2, 435 (1959)

[43] D.A. Varshalovich, A.N. Moskalev and V.K. Khersonskii *Quantum Theory of Angular Momentum*, World Scientific, Singapore, 1988

[44] V.N. Baier, Usp. Fiz. Nauk **105**, 441 (1971) [Sov. Phys.-Usp. 14, 695 (1972)]

[45] A.D. Kirsch, S.R. Mane, R.S. Raymond, T. Roser, J.A. Stewart, K.M. Terwilliger, B. Vuaridel, J.E. Goodwin, H.-O. Meyer, M.G. Minty, P.V. Pancella, R.E. Pollock, T. Rinckel, M.A. Ross, F. Sperisen, E.J. Stephenson, E.D. Courant, S.V. Lee and L.G. Ratner Phys. Rev. Lett. 63, 1137 (1989)